Reproducibility and Accuracy of Gated SPECT for Determination of Left Ventricular Volumes and Ejection Fraction: Experimental Validation Using MRI

Enrique Vallejo, Donald P. Dione, Wendy L. Bruni, R. Todd Constable, Peter P. Borek, Jason P. Soares, John G. Carr, Spyros G. Condos, Frans J.Th. Wackers, and Albert J. Sinusas

Experimental Nuclear Cardiology Laboratory, Division of Cardiovascular Medicine, Department of Internal Medicine; Department of Diagnostic Radiology; and Department of Surgery, School of Medicine, Yale University, New Haven, Connecticut

Quantitative gated SPECT (QGS) has been used for computation of left ventricular volumes and ejection fraction. This study evaluated, first, the effect of injected dose, time of imaging, and background activity on the reproducibility of QGS and, second, the accuracy of QGS, compared with cine MRI, for determining left ventricular volumes and ejection fractions in dogs with and without perfusion defects. **Methods:** Sixteen dogs were subjected to either chronic occlusion of the circumflex artery (group I, no perfusion defect) or acute occlusion of the anterior descending coronary artery (group II, perfusion defect). Both groups underwent serial MRI and SPECT. **Results:** QGS was very reproducible using the automated program ($r = 0.99997$). Correlation between left ventricular ejection fraction (LVEF) at 15 and 45 min was poor after the low-dose injection ($r = 0.54$; SE = 9%) and only fair after the high-dose injection ($r = 0.77$; SE = 5%). Correlation was poor in the presence of significant background activity ($r = 0.36$; SE = 12%). Correlation between QGS left ventricular volumes and MRI was good for group I (end-diastolic volume, $r = 0.86$; end-systolic volume, $r = 0.81$) and only fair for group II (end-diastolic volume, $r = 0.66$; end-systolic volume, $r = 0.69$). The overall LVEF correlation between QGS and MRI was poor ($r = 0.51$). QGS LVEF (mean ± SD, 42% ± 3%) overestimated MRI LVEF (29% ± 2%). **Conclusion:** QGS provides a highly reproducible estimate of LVEF. However, QGS is affected by changes in background activity, time of imaging, and injected dose. In the presence of perfusion defects, QGS overestimated volume relative to MRI. The correlation between QGS- and MRI-derived LVEF was poor in this canine model.

Key Words: MRI; left ventricular ejection fraction; electrocardiography-gated SPECT

Imaging with SPECT has been widely accepted for quantification of relative myocardial perfusion (*1,2*). Re-

cently, electrocardiography-gated SPECT has been proposed as an approach for quantification of global and regional left ventricular function (*3–12*). Investigators have developed both count-based and geometry-based approaches for assessment of regional thickening and motion (*4,5*) and for determination of volumes and left ventricular ejection fraction (LVEF) (*6–10*). The addition of functional information to perfusion data with a minimum of added time, cost, or equipment is attractive.

To calculate LVEF and left ventricular volumes from SPECT images, one must segment endocardial boundaries from the 3-dimensional image sets. An automated commercial software program, quantitative gated SPECT (QGS) (Cedars-Sinai Medical Center, Los Angeles, CA), has become widely used for computation of ventricular volumes and ejection fraction (*6*). This algorithm is based on geometric analysis of the left ventricular endocardial surface. Analysis of electrocardiography-gated SPECT images with this software package has been reported to provide reliable estimates of left ventricular volumes and LVEF (*6–10*). However, rigorous validation of this approach remains incomplete.

Estimation of the endocardial surface with SPECT can be affected by changes in image resolution, extracardiac background activity, count statistics, and reconstruction parameters (*10*). The confounding effects of some of these variables were highlighted by Achtert et al. (*10*) in a phantom study evaluating QGS. In addition, the estimate of left ventricular volumes and LVEF from electrocardiography-gated SPECT may be confounded by the presence of a SPECT perfusion defect. The potential confounding effects of a perfusion defect were raised in a study by Johnson et al. (*11*) and discussed in an editorial by Bonow (*12*). The effects of these potentially confounding variables on the quantitative analysis of function and volumes with gated SPECT remain undefined.

Electrocardiography-gated cine 3-dimensional MRI of-

fers much higher spatial resolution than either planar imaging or SPECT. MRI provides a truly 3-dimensional assessment of all cardiac chambers and has become the gold standard for estimating cardiac volumes and global ventricular function (13,14). MRI provides several advantages over radionuclide ventriculography. Left ventricular volumes can be measured using MRI without correcting for tissue attenuation or concern about overlap of adjacent structures, such as the left atrium or right ventricle (15–17). Estimation of left ventricular volume or global function with the first-pass technique is technically challenging. This approach requires a tight bolus, stable cardiac rhythm, and adequate mixing within the cardiac chambers. The MRI approach provides a time-averaged assessment of the left ventricle similar to gated SPECT. Therefore, cine MRI offers a more reliable approach for validation of electrocardiography-gated SPECT for analysis of global left ventricular function and volumes than does other equilibrium blood pool imaging or first-pass imaging.

This study had 3 goals: to measure the intraobserver variability of a widely used QGS algorithm for the determination of LVEF; to ascertain the effect of injected dose and changes in extracardiac background activity, which are associated with delayed imaging time, on the reproducibility of QGS for the quantification of LVEF; and to compare end-diastolic volumes, end-systolic volumes, and LVEF calculated from QGS with those calculated from electrocardiography-gated MRI, in the presence and absence of a perfusion defect.

MATERIALS AND METHODS

The experiments were performed on 16 fasting adult mongrel dogs anesthetized with the approval of the Yale Animal Care and Use Committee, in compliance with the guiding principles of the American Physiological Society on research animal use. All dogs were anesthetized with intravenous sodium thiamylal (20 mg/kg), intubated, and mechanically ventilated on a respirator (Boyle model 50; Harris-Lake Inc., Cleveland, OH) with a mixture of 0.5%–2% halothane and 3 parts N_2O to 1 part O_2. The electrocardiogram was monitored continually with a limb lead. A foreleg vein was cannulated for administration of fluids, ^{99m}Tc-sestamibi, and medications.

The dogs were separated into 2 groups: group I (6 dogs) was subjected to a chronic ameroid occlusion of the circumflex coronary artery. These dogs had little or no resting or stress perfusion abnormality. They were used to assess intraobserver variability and the potential effects of the injected dose and extracardiac background activity on the reproducibility of QGS. In group II (10 dogs), the proximal left anterior descending coronary artery was acutely occluded with a snare ligature. This model produced a mild to severe perfusion defect. Groups I and II were combined to analyze the effect of a perfusion defect on estimation of left ventricular volumes and LVEF with QGS. This analysis involved a direct comparison with MR images.

Surgical Preparation

Group I. Under aseptic conditions, a left thoracotomy was performed in the fifth intercostal space. The proximal circumflex coronary artery was dissected free from the surrounding tissue, and an ameroid occluder was placed around the vessel. The chest was closed in layers, and the animal was allowed to recover. The ameroid produced a subtotal or total occlusion over 3 wk, resulting in a highly collateralized perfusion territory. Thus, group I dogs had little or no resting perfusion abnormality.

Group II. Under aseptic conditions, a left thoracotomy was performed in the fifth intercostal space, and the heart was suspended in a pericardial cradle. The proximal left anterior descending coronary artery was isolated after the first major diagonal branch for placement of a snare ligature. For imaging, gauze was placed between the liver and the diaphragm to displace the liver away from the heart. The pericardial cradle was released, and the chest was loosely closed after externalization of the snare occluder. Arterial pH, partial pressure of carbon dioxide, and partial pressure of oxygen were measured serially, and the ventilator was adjusted to maintain these parameters within the physiologic range. A femoral vein and both femoral arteries were isolated and cannulated for administering fluids and drugs, monitoring pressure, and sampling arterial blood.

Experimental Protocols

An electrocardiography limb lead was monitored continuously during MRI and used for gating. The heart rate was recorded before each image acquisition for group I dogs. For group II dogs, an 8-French pigtail was placed in the aortic arch for measurement of central aortic pressure during MRI. Both groups underwent serial electrocardiography-gated SPECT and MRI. All images were acquired within a 3-h period under stable hemodynamic conditions. Five of the 6 group I dogs underwent sequential SPECT and MRI on 2 different days separated by at least 1 wk. The remaining group I dog underwent sequential imaging during a single session. This procedure resulted in 11 SPECT and MR image pairs for analysis among group I dogs. The 10 group II dogs underwent SPECT and MRI on only 1 d. This procedure resulted in an additional 10 SPECT and MR image pairs. All images were acquired with the dogs under anesthesia, permitting repeated serial SPECT without the risk of confounding subject motion.

Group I. The experimental protocol for group I dogs is summarized in Figure 1. After cine 3-dimensional MRI, animals received both low-dose (370 MBq) stress and high-dose (740 MBq) rest ^{99m}Tc-sestamibi injections. The stress injection was performed during a 6-min adenosine infusion (300 µg/kg/min). SPECT images were acquired 15 and 45 min after each injection, allowing for the evaluation of the potentially confounding effects of changing background activity in determination of LVEF using QGS. A total of 44 images were acquired. Of these, 38 images were processed twice for determination of intraobserver variability. To assess the potential confounding effects of background activity, each image was visually inspected and prospectively classified as having excessive or minimal adjacent extracardiac activity. The rest images acquired 45 min after ^{99m}Tc-sestamibi injection were used to correlate LVEF derived from gated SPECT with that derived from MRI.

Group II. After the dogs were prepared for surgery, they were positioned in the scanner for cine 3-dimensional MRI. Imaging was begun 10 min after the occluder of the left anterior descending coronary artery was tightened. Immediately after imaging, ^{99m}Tc-sestamibi (925 MBq) was injected intravenously at rest, and SPECT was begun 45 min later.
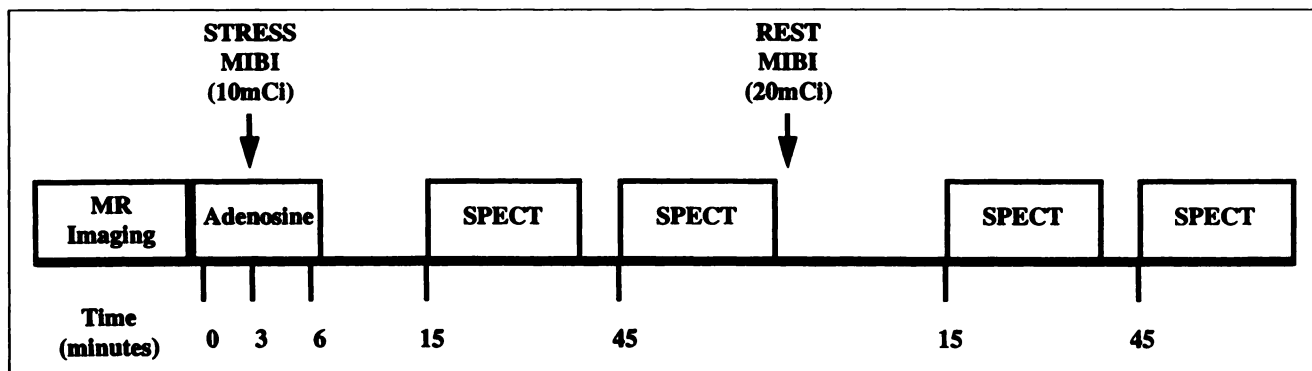
FIGURE 1. Experimental protocol. MIBI = sestamibi.

MR Image Acquisition and Analysis

MRI. MRI was performed in both groups on a Signa 1.5-T magnet (General Electric Medical Systems, Milwaukee, WI) with version 4.7 or 4.8 software, using the head coil (26-cm diameter) for transmission and reception. Short-axis images through the left ventricle were obtained with the gradient-echo cine technique using an echo time of 6 ms, a repetition time of 40 ms, and a flip angle of 30°. Sixteen phases were collected per cardiac cycle. For group I, 16 slices were collected in 2 separate acquisitions of 8 staggered 5-mm slices, with an overlap of 2 mm, a 256 × 256 matrix, and a 36-cm field of view, resulting in an in-plane resolution of 1.25 × 1.25 mm. For group II, 16 slices were collected in 4 sets of 4 nonoverlapping 5-mm slices, with a 256 × 256 matrix and a 42-cm field of view, resulting in an in-plane resolution of 1.64 × 1.64 mm.

MR Image Analysis. After each study, image analysis was performed off-line using Sparc 20 (Sun Microsystems, Inc., Mountain View, CA) and Octane (Silicon Graphics, Mountain View, CA) workstations. A previously reported semiautomated technique for left ventricular endocardial boundary segmentation that improves the reproducibility of surface contour generation was used (*18*). Endocardial contours were extracted from a series of contiguous short-axis MRI slices using a deformable contour-based segmentation. After defining the contours in the initial slice, the algorithm automatically propagated contours to adjacent slices. Defined contours were used as an initialization for the subsequent or preceding time frames; therefore, contours were also propagated through each time frame. All contours were reviewed and superimposed on their corresponding images and, if necessary, corrected using an image processing package developed in our laboratory on a Silicon Graphics workstation (*19*). The area enclosed by each contour was calculated and then multiplied by the effective slice thickness to give the volume of the slice. Finally, all the slice volumes were summed to give the chamber volume at each frame (*20*). Five MR images were processed twice to establish the reproducibility of our quantitative MRI analysis.

SPECT Image Acquisition and Analysis

SPECT. All SPECT images were acquired on a triple-head γ camera system (Prism 3000XP; Picker International, Inc., Bedford Heights, OH) equipped with high-resolution collimators. Electrocardiography-gated images were acquired at 16 frames per cardiac cycle, a rate that was comparable with the MR image acquisition. A matrix size of 64 × 64 pixels was used, resulting in a pixel size of approximately 5 mm in both the x and the y directions. All images were acquired with a 360° orbit and step-and-shoot protocol,

(60 s/image; 6°/stop). A 20% window was set symmetrically over the 140-keV photopeak of ^{99m}Tc. All images were reconstructed with standard filtered backprojection and a ramp filter. A postreconstruction low-pass (order, 4; cutoff, 0.25) 3-dimensional filter was applied. The reconstructed and processed short-axis images (5 mm thick) were transferred to a Sparc 20 workstation for off-line quantitative analysis.

SPECT Image Analysis. The SPECT perfusion images were quantified with computer software (Yale CQ) developed in our laboratory (*21*). Electrocardiography-gated images were summed before quantification. Standard circumferential count profiles were generated for each short-axis slice. Defect size was measured on each of the short-axis slices by integrating the area under a reference line at 80% of maximal counts. The defect nadir, defined as the point with the lowest counts on the circumferential profiles, was expressed as a percentage of maximal counts and provided a measure of defect severity.

Reconstructed electrocardiography-gated SPECT images were processed, and left ventricular volumes and LVEF were calculated, using the fully automated QGS software (*6*). The algorithm operates in 3-dimensional space. The software segments the left ventricle, estimates and displays the 3-dimensional surface defined by the endocardium and the valve plane, and calculates the left ventricular cavity volume as the sum of the voxel columns inside that surface without operator interactions. If the software failed, then manual or constrain analysis was performed. The manual mode allows the operator to define a region of interest around the epicardial borders. This region of interest excludes the extracardiac activity and restricts the search volume of the algorithm. Furthermore, the algorithm can be forced to use an operator-specified left ventricular long axis of the heart instead of the automated determination. The left ventricular long axis is defined by selecting the apex and base limits (constrain mode). These alternative approaches are operator dependent and therefore more subjective.

Statistical Analysis

Data are presented as the mean ± SEM. LVEF, end-diastolic, and end-systolic volumes determined by gated SPECT using QGS were compared with those derived from MRI in the same animals using linear regression analysis. Intraobserver agreement was evaluated using a similar linear regression analysis. The tightness of the fit was determined by evaluation of the SEE. A Bland-Altman plot was also used to assess systematic differences between SPECT- and MRI-derived parameters. Paired and unpaired Student

t tests were used to compare values within groups and between groups, respectively. *P* < 0.05 (2-tailed) was considered significant.

RESULTS

Hemodynamics

Hemodynamic parameters remained stable throughout the MRI and SPECT period. Group I dogs showed no difference in heart rate during MRI and SPECT. Group II dogs showed no significant change in either heart rate or blood pressure.

Determination of Perfusion Defect Size

Perfusion defect size was computed for summed SPECT images. Group I dogs had little or no perfusion defect either at rest or during stress. The average defect nadir (± SD) was 78% ± 2% of the maximum for group I stress images. The average defect nadir for the rest images was 75% ± 2% of the maximum, which was not significantly different. In contrast, the group II dogs had moderate rest defects involving approximately 25% of the left ventricle, with a defect nadir of 22% of the maximum.

Quantification of LVEF with QGS

Assessment of Intraobserver Variability. Thirty-eight images from group I were processed twice to establish the reproducibility of QGS for determination of LVEF. Half the images were acquired 15 min after injection, and half were acquired 45 min after injection. In processing 30 of 38 images, the automated program succeeded both times. When the automated program succeeded (30 pairs), the reproducibility was high (*r* = 0.99997) (Fig. 2A). The automated program failed 21% of the time, and the analysis needed to be constrained. Generally, these failures could be attributed to adjacent extracardiac background activity. Although the reproducibility of the constrained method was also high (*r* = 0.96) (Fig. 2B), the LVEF derived using the constrained analysis was consistently lower than the MRI-derived LVEF (MRI LVEF [n = 30], 43% ± 10%; constrained LVEF [n = 8], 30% ± 12%; *P* = 0.007).

Effect of Injected Dose and Delay in Imaging Time. The effect of injected dose and delay in imaging time for group I is illustrated in Figure 3. QGS was applied to images

acquired 15 and 45 min after injection. The correlation between LVEF determined 15 and 45 min after the low-dose stress images was poor (*r* = 0.54; SE = 9%) (Fig. 3A). The correlation between LVEF determined 15 and 45 min after the high-dose resting images was only fair (*r* = 0.77; SE = 5%) (Fig. 3B). Therefore, determination of LVEF using QGS on 2 images separated by only 30 min was poorly reproducible. The reproducibility of QGS for determination of LVEF between early (15 min) and delayed (45 min) images was better for high-dose rest images.

Effects of Extracardiac Background Activity. To better understand the observed discrepancy in the calculation of LVEF using QGS, we prospectively classified images on the basis of background activity adjacent to the heart (Fig. 4). Each image pair was classified as having excessive extracardiac activity; minimal activity; or, if only 1 image of the pair had excessive background activity, mixed activity. Sixteen image pairs were prospectively judged to have excessive extracardiac activity at both 15 and 45 min. When extracardiac background activity was judged to be excessive on both images, the correlation was poor (*r* = 0.36; SE = 12%) (Fig. 4A). Extracardiac activity was judged to be minimal on 15 image pairs. When extracardiac activity was judged to be minimal, the reproducibility was good (*r* = 0.89; SE = 4%) (Fig. 4B). A Bland-Altman plot revealed no systematic difference in error over the entire range of LVEFs evaluated.

Reproducibility of MRI Analysis

The reproducibility of our MRI analysis for determination of left ventricular end-systolic and end-diastolic volume and LVEF was evaluated for 5 MR images completely processed twice. The correlation coefficients for MRI-determined end-diastolic and end-systolic volumes were high, at 0.997 and 0.98, respectively. The average LVEF was identical for both determinations (36.2% ± 2.9% for end-diastolic volume and 36.4% ± 1.5% for end-systolic volume).

Correlation Between QGS and Cine 3-Dimensional MRI

Correlation Between Gated SPECT and MRI of End-Diastolic Volumes. The observed correlation between MRI- and QGS-determined left ventricular end-diastolic volume
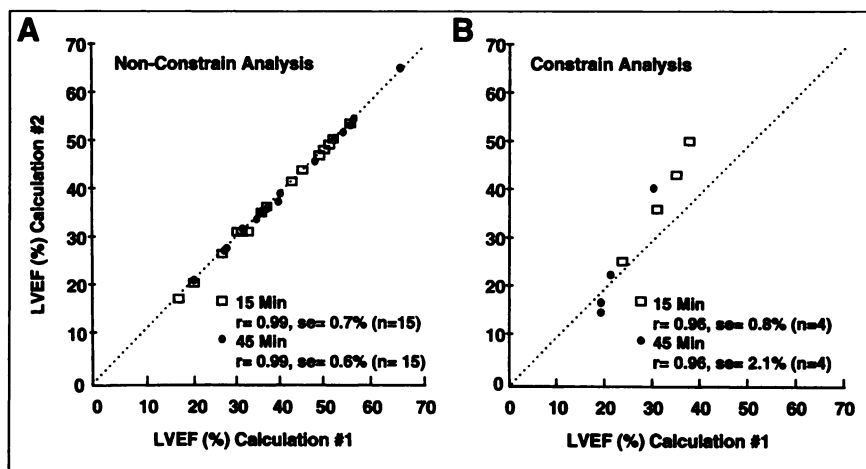

FIGURE 2. Intraobserver variability of QGS for determination of LVEF. Images were acquired 15 (□) and 45 (●) min after injection. (A) Thirty images were processed both times without having to apply constrained algorithm. Automated program was highly reproducible. (B) Automated program failed in processing 8 images, and analysis needed to be constrained. Program was also reproducible if constrained analysis was required.

FIGURE 3. Effect of dose and delay in imaging on reproducibility of QGS. Images were acquired 15 (x-axis) and 45 (y-axis) min after low-dose stress (A) and high-dose rest (B) injection. Correlation for low-dose stress images was poor ($r = 0.54$), with high SE of 9%. Correlation for high-dose images was only fair ($r = 0.77$).
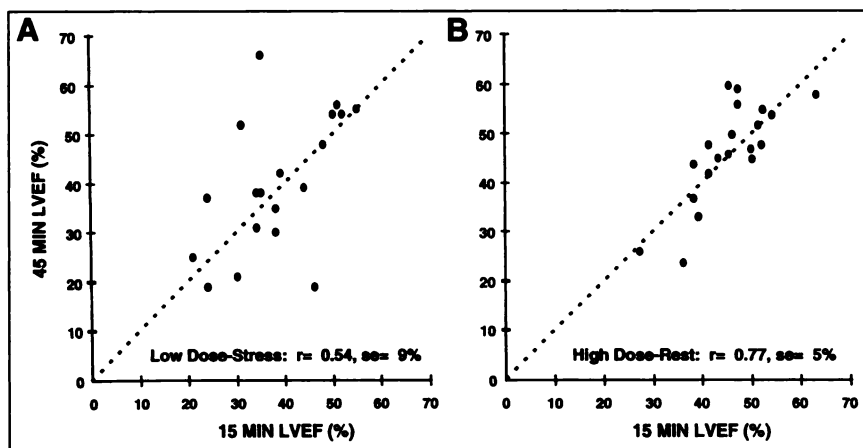
for group I and II dogs is shown in Figure 5. The correlation of end-diastolic volume was good ($r = 0.86$; SE = 7) for group I dogs. However, the correlation between MRI- and QGS-determined end-diastolic volume was only fair ($r = 0.66$; SE = 8) for group II dogs. In both groups, the average QGS end-diastolic volume was significantly greater than the MRI end-diastolic volume ($P < 0.01$ and $P < 0.00001$, respectively). The overestimation was much worse for group II dogs. In this group, the QGS end-diastolic volume was 59 ± 5 mL, whereas the MRI volume was only 36 ± 3 mL.

Correlation Between Gated SPECT and MRI of End-Systolic Volumes. The observed correlation between MRI- and QGS-determined left ventricular end-systolic volume was good for group I dogs ($r = 0.81$; SE = 6) and less favorable for group II dogs ($r = 0.69$; SE = 6) (Fig. 6). Although QGS tended to overestimate left ventricular end-diastolic volume in group I, the end-systolic volume was not significantly different in these dogs. In group II, end-systolic volume derived using QGS was significantly larger than MRI-derived end-systolic volume ($P < 0.01$).

Correlation Between Gated SPECT and MRI LVEF

The observed correlation between MRI and gated SPECT for determination of LVEF is illustrated in Figure 7. The overall correlation between gated SPECT and MRI for determination of LVEF was only fair ($r = 0.51$; SE = 8)

over a wide range of ejection fractions (9%–48%). The correlation was poor when both groups were analyzed separately. The average QGS-derived LVEF (42% $\pm$ 3 mL) significantly overestimated the MRI-derived LVEF (29% $\pm$ 2 mL) ($P < 0.0001$).

DISCUSSION

Electrocardiography-gated SPECT allows simultaneous assessment of both perfusion and function. Several approaches for analysis of left ventricular volume and LVEF using electrocardiography-gated SPECT have been developed. QGS is a widely used commercial program for the estimation of LVEF and cardiac volumes from gated SPECT perfusion studies (6). Although this automated program has been extensively evaluated (6–12), several conditions may affect the accuracy of the program (10–12). Bonow (12) suggested that a perfusion defect could result in misidentification of the endocardial surface and underestimation of left ventricular function after a stress injection. Achtert et al. (10), using phantom studies, showed the potentially confounding effects of extracardiac background activity and signal-to-noise ratio on the accuracy of QGS. The automated QGS program often failed in the presence of excessive background activity.

We postulated that the accuracy of electrocardiography-

FIGURE 4. Effect of background on reproducibility of QGS for determination of LVEF. Images were classified as having excessive or minimal background activity. (A) When background was judged to be excessive, correlation was poor ($r = 0.36$). (B) When background was minimal, reproducibility was good ($r = 0.89$).
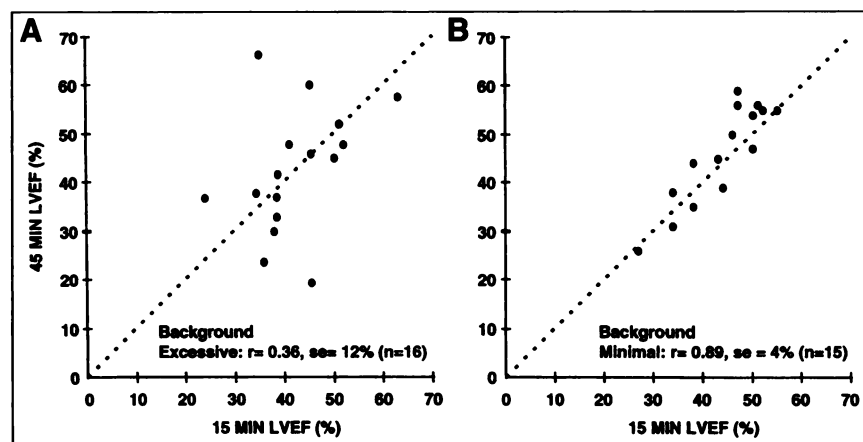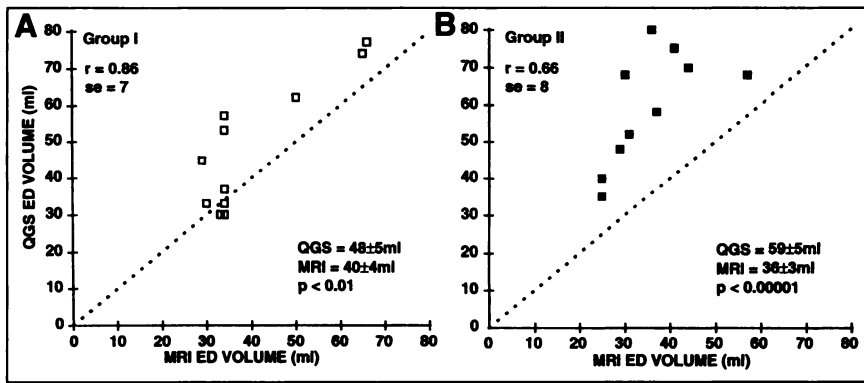
FIGURE 5. Correlation between MRI and gated SPECT end-diastolic (ED) volumes (in milliliters) for both group I (A) and group II (B) dogs. Dashed line represents line of identity. Correlation for ED volume was good ($r = 0.86$) in absence of perfusion defect (group I). In presence of perfusion defect (group II), correlation was only fair ($r = 0.66$). In both groups, QGS overestimated MRI volume.

gated SPECT for determination of left ventricular volumes and LVEF would be affected by changes in background activity, the presence of a perfusion defect, the injected dose, and acquisition and reconstruction parameters. To evaluate these issues, we performed serial gated SPECT in dogs with and without perfusion defects and compared the results from QGS with quantitative 3-dimensional cine MR images. The reproducibility and accuracy of QGS for estimation of left ventricular volume and LVEF were significantly affected by the injected dose and a delay in imaging. The observed variability was, in part, related to changes in extracardiac background activity and the presence of a perfusion defect. QGS tended to overestimate LVEF relative to MRI-determined values, particularly in the presence of a perfusion defect.

Reproducibility of QGS and Background Effects

This study confirms that automated determination of LVEF from gated SPECT using QGS provides a highly reproducible estimate of LVEF on the same image. This finding was expected, because the program is fully automated and does not require manual edge delineation. However, a 30-min delay in image acquisition after injection significantly affected the determination of LVEF. The variability in LVEF associated with a delayed imaging time can be attributed to changes in extracardiac background activity. In clinical practice, SPECT is typically started 30–60 min after a resting injection. These standard delays in imaging may significantly affect the reproducibility of QGS for determination of LVEF.

When extracardiac uptake (liver or gut) was similar in intensity to cardiac uptake, the automated program was unable to identify the left ventricle. The contour inappropriately included the adjacent organ and therefore incorrectly estimated left ventricular volumes. Manual correction of this error led to systematic underestimation of LVEF.

The effects of background activity on LVEF estimation by gated SPECT have been analyzed previously. Marcassa et al. (22) showed that an increase in the background activity induced a false reduction in measured wall thickening. Achtert et al. (10) also showed the potential confounding effects of background activity, using phantom studies. We have shown that small changes in background activity associated with a delay in imaging time can affect the calculation of left ventricular volume and LVEF using QGS. The animal model we used allowed us to perform in vivo serial gated SPECT studies without the confounding effects of motion.

Dose Effects

The reproducibility of QGS for estimation of LVEF was also affected by the dose of radioactivity injected. A weaker correlation was observed for the low-dose images than for the high-dose images. The injected dose influences the statistical quality of the image. Presumably, a higher dose would lead to more favorable count statistics within the heart and better image resolution. Achtert et al. (10) analyzed the effect of variation in count statistics on LVEF estimation and showed that the SD of LVEF values increases as count levels decrease. In addition, lower counts lead to
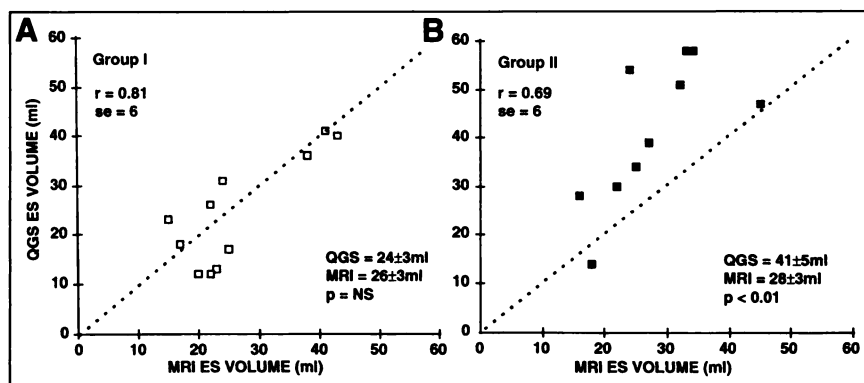

FIGURE 6. Correlation between MRI and gated SPECT end-systolic (ES) volumes (in milliliters) for both group I (A) and group II (B) dogs. Correlation of ES volume was good ($r = 0.81$) in absence of perfusion defect (group I). In presence of perfusion defect (group II), correlation was only fair ($r = 0.69$) and QGS overestimated ES volume.
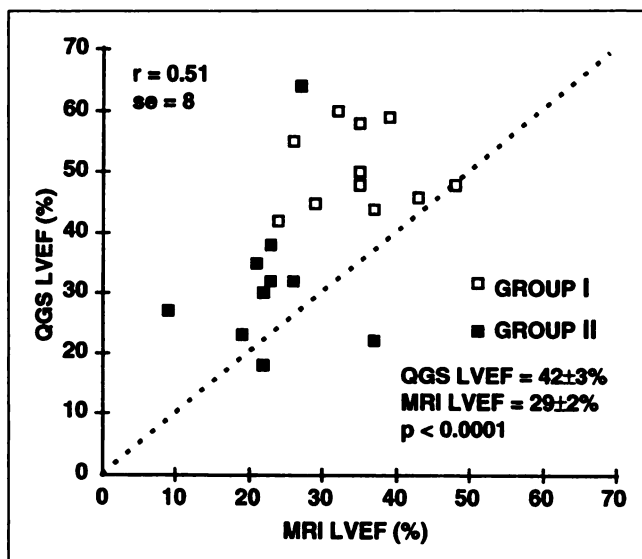
FIGURE 7. Correlation between MRI and gated SPECT LVEF for group I (□) and group II (■) dogs. Overall, correlation was poor (r = 0.51) between MRI- and QGS-determined LVEF for all dogs. QGS significantly overestimated MRI-derived LVEF.

increased image noise and may affect the accuracy of edge definition. Noise filtering has been shown to increase the calculated LVEF in patients with small hearts (23). Pretorius et al. (24) found that attenuation correction improved the accuracy of edge definition. They attributed this improvement to regional alteration of counts and improved signal-to-noise ratio.

Effect of Defect Size on Accuracy of QGS

We compared left ventricular volumes and LVEF derived using QGS and cine 3-dimensional MRI in dogs with and without perfusion defects. QGS overestimated the end-diastolic volumes in the presence and absence of a perfusion defect. However, the overestimation was worse in the presence of a perfusion defect. End-systolic volume was also overestimated by QGS in the presence of a perfusion defect. QGS overestimated LVEF compared with quantitative MRI, particularly in the presence of a perfusion defect. This difference can be attributed to the absence of tracer activity in the myocardial wall, compromising the edge detection component of the program and forcing the fitting of geometrically determined contours to the defect area. This geometric assumption is based on normal left ventricular shapes, which cannot reliably be used in these distorted ventricles. Previous studies using geometric approaches have reported similar findings in patients with perfusion defects (11,25,26).

Count-Based Versus Geometry-Based Analysis

Several radionuclide methods have been proposed to determine cardiac volumes, including count-based distance methods (27,28), count-based ratio methods (29,30), and geometric methods (13,31). The disadvantages of geometric methods include the limited resolution of SPECT and the use of a prolate ellipsoid model. The shape of the normal left

ventricle may be approximated by the ellipsoid model; however, in pathologic conditions the left ventricle may be asymmetrically deformed, and use of this geometric model may no longer be appropriate. Count-based distance methods are subject to variations in background activity, attenuation, and scatter. Count-based ratio methods also depend on accurately finding the highest count pixel, which is influenced by the viewing angle of the left ventricle and noise in the image (32).

The automated QGS approach defines the endocardial and epicardial surfaces on the basis of an asymmetric gaussian system fit of the midmyocardial count distribution profile and also assumes a geometric model (6). Although QGS takes advantage of the strengths of each of these approaches, the method also suffers from disadvantages associated with each approach.

MRI as a Gold Standard for Assessment of Left Ventricular Volumes and LVEF

Most of the earlier validation studies of QGS used first-pass angiography (6) or equilibrium radionuclide ventriculography (9). In our study, the accuracy of QGS for estimation of left ventricular volumes and LVEF was evaluated by a direct comparison with values derived from MRI. MRI offers several advantages for estimation of volume, and the accuracy of cine MRI volumes has been validated in dogs. Cine MRI also has been well validated for assessment of left ventricular function in both normal and dilated ventricles. MRI provides improved resolution and 3-dimensional imaging with no geometric assumptions to determine ventricular dimensions (5,33,34). In our comparisons of QGS with cine MRI, we found only a fair correlation for determination of end-diastolic volumes, end-systolic volumes, and LVEF. These relationships were worse in dogs with a perfusion defect. A patient study of Iskandrian et al. (8) that showed a poor correlation (r = 0.58) between stroke volume determined using QGS and stroke volume determined using thermodilution techniques supports our observations.

Study Limitations

This study has several limitations. The small size of the canine hearts may have affected the results, secondary to a partial-volume effect associated with the low resolution of SPECT. The partial-volume error could have led to an underestimation of left ventricular volume, particularly at end-systole, when the left ventricular cavity was smallest. Interestingly, Kang et al. (35) recently reported the normal range of end-systolic volumes in male and female patients with a low likelihood of coronary artery disease using QGS. End-systolic volumes (male patients, 37.4 ± 13.7 mL; female patients, 21.1 ± 11.0 mL) were comparable with those determined in our canine model using both MRI and QGS.

We did not assess the accuracy of this approach with perfusion abnormalities in regions other than those supplied by the left anterior descending coronary artery. An alterna-

tive location for the perfusion defect might have impaired the correlation. The program may more easily compensate for smaller defects that do not include the apex. In contrast, a regional perfusion defect in a basal segment may impair the estimation of the valve plane and alter the estimation of LVEF. Further studies are warranted to evaluate the accuracy of the program when perfusion abnormalities are in different regions and are of different sizes and severities.

A transient period of myocardial stunning may have occurred in group I dogs during infusion of adenosine. Therefore, changes in LVEF over time may represent recovery from stress-induced left ventricular dysfunction over time. This potential effect is unlikely, because significant perfusion defects were not observed in these animals either at rest or during stress. If the dogs were stunned, we should have observed a reversible perfusion defect caused by a partial-volume error in the dysfunctional area (36,37).

Clinical Implications

Global left ventricular function is a major predictor of prognosis in patients with ischemic heart disease (38). The incremental value of adding qualitative information about myocardial contractile function to perfusion has been established (39,40). Although the accuracy of gated SPECT techniques for estimation of left ventricular function has been reasonable in several clinical studies, some issues remain unresolved. Electrocardiography-gated SPECT analysis of function and volume may be affected by injected dose, timing of imaging, background activity, and presence of a perfusion defect. In this canine model, we showed that QGS overestimated end-diastolic volume relative to end-systolic volume; consequently, QGS overestimated LVEF compared with quantitative MRI. Investigators need to consider these issues when reviewing the results of quantitative electrocardiography-gated SPECT analysis over time. In particular, the reliability of QGS should be considered with reference to the presence of potentially confounding extracardiac background activity and large perfusion defects.

CONCLUSION

In this study we showed, at best, a fair correlation between QGS and MRI for determining LVEF in this canine model. Compared with MRI, QGS provided a reasonable estimate of left ventricular volumes in the absence of a perfusion defect. However, QGS was less accurate in the presence of a perfusion defect. Although this automated method was highly reproducible when applied to the same image, considerable variability was seen in the estimation of LVEF on serial images. Estimation of left ventricular volume and LVEF using gated SPECT can be significantly affected by changes in background activity, dose of radioactivity injected, and presence of a perfusion defect. Therefore, further clinical investigation of these potentially confounding variables is warranted.

REFERENCES

1. Ritchie JL, Bateman TM, Bonow RO, et al. Guidelines for clinical use of cardiac radionuclide imaging: report of the American College of Cardiology/American Heart Association Task Force on assessment of diagnostic and therapeutic cardiovascular procedures (Committee on Radionuclide Imaging), developed in collaboration with the American Society of Nuclear Cardiology. *J Am Coll Cardiol.* 1995;25:521–547.
2. Kiat H, Maddahi J, Roy LT, et al. Comparison of technetium-99m methoxy-isobutyl-isonitrile and thallium-201 for evaluation of coronary artery disease by planar and tomographic methods. *Am Heart J.* 1989;117:1–11.
3. Mannting F, Morgan-Mannting MA. Gated SPECT with technetium 99m sestamibi for assessment of myocardial perfusion abnormalities. *J Nucl Med.* 1993;34:601–608.
4. DePuey EG, Rozanski A. Using gated technetium 99m sestamibi SPECT to characterize fixed myocardial defects as infarct or artifact. *J Nucl Med.* 1995;36:952–955.
5. Ziffer J, Cooke C, Folks R, LaPidus A, Alzaraki N, Garcia E. Quantitative myocardial thickening assessed with sestamibi: clinical evaluation of a count-based method [abstract]. *J Nucl Med.* 1991;32(suppl):1006.
6. Germano G, Kiat H, Davanagh PD, et al. Automatic quantification of ejection fraction from gated myocardial perfusion SPECT. *J Nucl Med.* 1995;36:2138–2147.
7. Germano G, Kavanagh PB, Kavanagh JT, Wishner SH, Berman DS, Kavanagh GJ. Repeatability of automatic left ventricular cavity volume measurements from myocardial perfusion SPECT. *J Nucl Cardiol.* 1998;5:477–483.
8. Iskandrian AE, Germano G, VanDecker W, et al. Validation of left ventricular volume measurements by gated SPECT ^{99m}Tc-labeled sestamibi imaging. *J Nucl Cardiol.* 1998;5:574–578.
9. Everaert H, Bssuyt A, Franken PR. Left ventricular ejection fraction and volumes from gated single photon emission tomographic myocardial perfusion images: comparison between two algorithms working in three-dimensional space. *J Nucl Cardiol.* 1997;4:472–476.
10. Achtert AD, King MA, Dahlberg ST, Hendrik P, LaCroix KJ, Tsui BMW. An investigation of the estimation of ejection fractions and cardiac volumes by quantitative gated SPECT software package in simulated gated SPECT images. *J Nucl Cardiol.* 1998;5:144–152.
11. Johnson LL, Verdesca SA, Aude WY, Xavier RC, Nott LT, Campanella MW. Postischemic stunning can affect left ventricular ejection fraction and regional wall motion on post-stress gated sestamibi tomograms. *J Am Coll Cardiol.* 1997;30:1641–1648.
12. Bonow RO. Gated myocardial perfusion imaging for measuring left ventricular function. *J Am Coll Cardiol.* 1997;30:1649–1650.
13. Møgelvang J, Thomsen C, Mehlsen J, Bräckle G, Stubgaard M, Henriksen O. Evaluation of left ventricular volumes by magnetic resonance imaging. *Eur Heart J.* 1986;258:1181–1186.
14. Pattynama PMT, De Roos A, Van der Wall EE, Van Voorthuisen AE. Evaluation of cardiac function with magnetic resonance imaging. *Am Heart J.* 1994;128:595–607.
15. Johnson LL, Lawson MA, Blackwell GG, Tauxe EL, Russell K, Dell'Italia LJ. Optimizing the method to calculate right ventricular ejection fraction from first-pass data acquired with a multicrystal camera. *J Nucl Cardiol.* 1995;2:372–379.
16. Sechtem U, Pflugfelder PW, Gould RG, Cassidy MM, Higgins CB. Measurement of right and left ventricular volumes in healthy individuals with cine MR imaging. *Radiology.* 1987;163:697–702.
17. Gunning MG, Anagnostopoulos C, Davies G, Forbat SM, Ell PJ, Underwood SR. Gated technetium-99m-tetrofosmin SPECT and cine MRI to assess left ventricular contraction. *J Nucl Med.* 1997;38:438–442.

18. Chakrabarty A, Staib LH, Duncan JS. Deformable finding in medical images by integrating gradient and region information. *IEEE Trans Med Imaging.* 1996;15: 859–870.

19. Papademetris X, Rambo J, Dione DP, Sinusas AJ, Duncan JS. Visually interactive semi-automated segmentation of cine magnetic resonance images [abstract]. *J Am Coll Cardiol.* 1998;31(suppl):7A.

20. Edelman RR, Thompson R, Kantor H. Cardiac function: evaluation with fast-echo MR imaging. *Radiology.* 1987;162:611–615.

21. Liu YH, Sinusas AJ, DeMan P, Zaret BL, Wackers FJT. Quantification of SPECT myocardial perfusion images: methodology and validation of the Yale-CQ method. *J Nucl Cardiol.* 1999;6:190–204.

22. Marcassa C, Marzullo P, Parodi O, Sambuceti G, L'Abbate A. A new method for noninvasive quantitation of segmental myocardial wall thickening using technetium-99m 2-methoxy-isobutyl-isonitrile scintigraphy: results in normal subjects. *J Nucl Med.* 1990;31:173–177.

23. Case JA, Cullom SJ, Bateman TM, Barnhart C, Saunders MJ. Overestimation of LVEF by gated MIBI myocardial perfusion SPECT in patients with small hearts [abstract]. *J Am Coll Cardiol.* 1998;31(suppl A):43A.

24. Pretorius PH, Xia W, King MA, Tsui B, Pan TS, Villegas BJ. Evaluation of right and left ventricular volume and ejection fraction using a mathematical cardiac torso phantom. *J Nucl Med.* 1997;38:1528–1535.

25. Williams KA, Taillon LA. Left ventricular function in patients with coronary artery disease assessed by gated tomographic myocardial perfusion images. *J Am Coll Cardiol.* 1996;27:173–181.

26. DePuey EG, Nichols K, Dobrinsky C. Left ventricular ejection fraction assessed from gated technetium-99m-sestamibi SPECT. *J Nucl Med.* 1993;34:1871–1876.

27. Calnon DA, Kastner RJ, Smith WH, Segalla D, Beller GA, Watson DD. Validation of a new counts-based gated single photon emission computed tomography method for quantifying left ventricular systolic function: comparison with equilibrium radionuclide angiography. *J Nucl Cardiol.* 1997;4:464–471.

28. Strauss HW, Zaret BL, Hurley PJ, Natarajan TK, Pitt B. A scintiphotographic method for measuring left ventricular ejection fraction in man without cardiac catheterization. *Am J Cardiol.* 1971;28:575–580.

29. Wackers FJT, Berger HJ, Johnstone DE, et al. Multiple gated cardiac blood pool imaging of left ventricular ejection fraction: validation of the technique and assessment of variability. *Am J Cardiol.* 1979;43:1159–1166.

30. Massardo T, Gal RA, Grenier RP, Schmidt DH, Port SC. Left ventricular volume calculation using a count-based ratio method applied to multigated radionuclide angiography. *J Nucl Med.* 1990;31:450–456.

31. Najm YC, Timmis AD, Maisey MN, et al. The evaluation of left ventricular function using gated myocardial imaging with Tc-99m MIBI. *Eur Heart J.* 1989;10:142–148.

32. Levy WC, Cerqueira MD, Matsuoka DT, Harp GD, Sheehan FH, Stratton JR. Four radionuclide methods for left ventricular volume determination: comparison of a manual and an automated technique. *J Nucl Med.* 1992;33:763–770.

33. Møgelvang J, Lindvig K, Sondergaard L, Saunamaki K, Henriksen O. Reproducibility of cardiac volume measurements including left ventricular mass determined by MRI. *Clin Physiol.* 1993;13:587–597.

34. Markiewicz W, Sechtem U, Kirby R, Derugin N, Caputo GC, Giggins CB. Measurement of ventricular volumes in the dog by nuclear magnetic resonance imaging. *J Am Coll Cardiol.* 1987;10:170–177.

35. Kang X, Berman DS, Germano G, et al. Normal parameters of left ventricular volume and ejection fraction measured by gated myocardial perfusion SPECT [abstract]. *J Am Coll Cardiol.* 1999;33(suppl):409A.

36. Eisner RL, Schmarkey S, Martin SE, et al. Defects on SPECT "perfusion" images can occur due to abnormal segmental contraction. *J Nucl Med.* 1994;35:638–643.

37. Sinusas AJ, Shi Q, Vitols PJ, et al. Impact of regional ventricular function, geometry, and dobutamine stress on quantitative 99mTc-sestamibi defect size. *Circulation.* 1993;88:2224–2234.

38. Pfeffer MS, Braunwald E. Ventricular enlargement and remodelling after myocardial infarction: experimental observations and clinical implications. *Circulation.* 1990;81:1161–1172.

39. The Multicenter Postinfarct Research Group. Risk stratification and survival after myocardial infarction. *N Engl J Med.* 1983;309:331–336.

40. White HD, Norris RM, Brown MA, Brandt PWT, Whitlock RML, Wild CJ. Left ventricular end-systolic volume as a major determinant of survival after recovery from myocardial infarction. *Circulation.* 1987;76:44–51.